

## 11.2

## Drag of Two-Dimensional Bodies

### Drag of a Thin Plate

To illustrate the relative effect of pressure and viscous forces on drag, we shall consider the drag of a plate first oriented parallel to the flow and then oriented normal to the flow. In the parallel position, the only force acting is viscous shear in the direction of the flow. Hence, from our considerations of surface resistance in Chapter 9, the drag for both sides of the plate is given as

$$F_D = 2C_f b \ell \rho \frac{V_0^2}{2} \rightarrow \text{[Diagram of a plate in flow]}$$

When the plate is turned normal to the flow, as in Fig. 11.3, both pressure and viscous forces act on the plate. However, the viscous forces act only in the transverse direction and, in addition, are symmetrical about the midpoint of the plate. Consequently, the viscous forces do not directly contribute to the lift or drag of the plate. Because the pressure on the plate acts to produce a force only in a direction parallel to the flow, the pressure force contributes totally to the drag of the body. Hence Eq. (11.2) applied to the plate reduces to

$$F_D = \int (-p \cos \theta) dA$$

The pressures on the upstream and downstream sides of the plate can be obtained experimentally and are usually given in terms of  $C_p$ , as shown in Fig. 11.4 for flow with a relatively high value of the Reynolds number ( $V_0 b / \nu > 10^4$ ).

Since the pressure on the downstream side is essentially constant,

$$p = p_0 - 1.2 \rho \frac{V_0^2}{2}$$

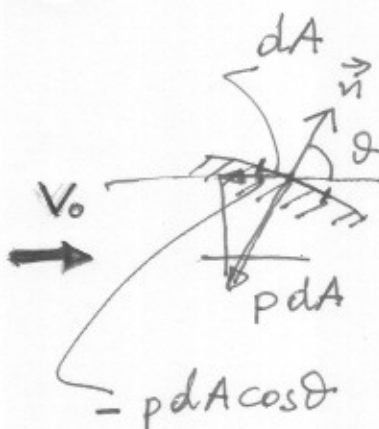


FIGURE 11.3

Flow past a flat plate.

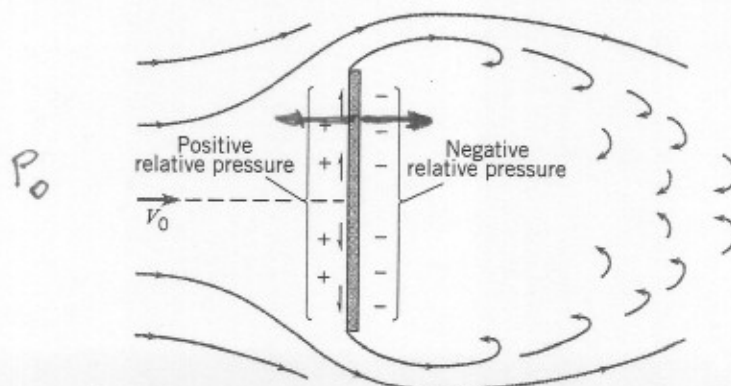
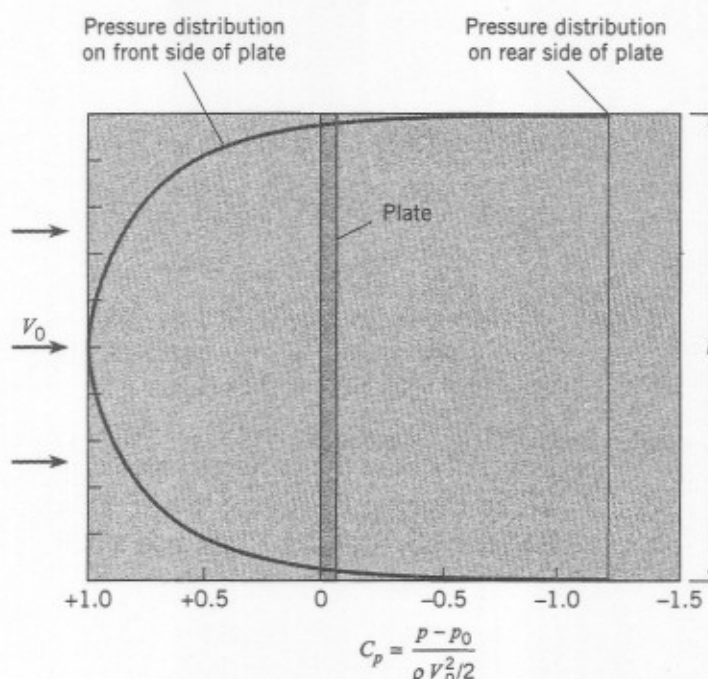


FIGURE 11.4

Pressure distribution on a plate normal to the approach flow for  $Re > 10^4$ .



and since  $\theta = 0$ , the contribution to drag for the downstream side is

$$\mathcal{J}=0 \quad F_{D, \text{downstream}} = -\left(p_0 - 1.2\rho\frac{V_0^2}{2}\right)b\ell = -p_0b\ell + 1.2\rho\frac{V_0^2}{2}b\ell$$

where  $\ell$  is the length of the plate normal to the plane of the paper, and by definition of a two-dimensional body,  $\ell \gg b$ . For the front side,  $\theta = \pi$ . Hence  $\cos \theta = -1$ , and the contribution to drag due to pressure on the upstream side is

$$\mathcal{J}=\pi \quad F_{D, \text{upstream}} = \int_{-b/2}^{b/2} \left(p_0 + C_p\rho\frac{V_0^2}{2}\right)\ell dy = p_0b\ell + \rho\frac{V_0^2}{2}\ell \int_{-b/2}^{b/2} C_p dy$$

Then the total drag on the plate is given by

$$\begin{aligned} F_D &= F_{D, \text{upstream}} + F_{D, \text{downstream}} \\ &= \rho\frac{V_0^2}{2}\ell \left( \int_{-b/2}^{b/2} C_p dy + 1.2b \right) \end{aligned} \quad (11.3)$$

Evaluation of the first term inside the parentheses on the right-hand side of Eq. (11.3) yields a magnitude of approximately  $0.8b$ . Thus the drag of this plate is given as

$$F_D = \rho\frac{V_0^2}{2}b\ell(0.8 + 1.2) \quad (11.4)$$

We must take note of the pure numbers inside the parentheses of Eq. (11.4). The number 0.8 in Eq. (11.4) represents the average pressure coefficient  $C_p$  over the upstream side of the plate. In fact, the sum inside the parentheses ( $0.8 + 1.2$ )

of this equation reflects the manner in which the pressure is distributed over the upstream side and downstream side of the body. Because the drag varies directly with the magnitude of this quantity, it has been appropriately defined as the *coefficient of drag*  $C_D$ . Thus Eq. (11.4) can be written as

$$F_D = C_D A_p \rho \frac{V_0^2}{2} \quad (11.5)$$

where  $C_D$  is the coefficient of drag,  $A_p$  is the projected area of the body,  $\rho$  is the fluid density, and  $V_0$  is the free-stream velocity. The projected area  $A_p$  is the silhouetted area that would be seen by a person looking at the body from the direction of flow. For example, the projected area of the above plate normal to the flow is  $b\ell$ , and the projected area of a cylinder with its axis normal to the flow is  $d\ell$ . In Chapter 8 we saw that  $C_p$  is a function of the Reynolds number  $Re$ ; and because  $C_D = f(C_p)$ ,  $C_D$  is also a function of  $Re$ . When the drag of bodies is due solely to the shear stress on the body,  $C_D$  is still a function of  $Re$  because  $\tau$  is also a function of  $Re$ .

### Coefficients of Drag for Various Two-Dimensional Bodies

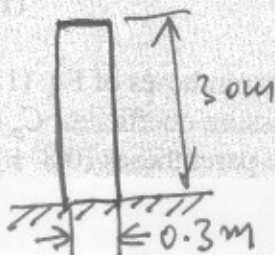
We have already seen that  $C_D$  can be determined if the pressure and shear-stress distribution around a body are known. The coefficient of drag can also be calculated if the total drag is measured, for example, by means of a force balance in a wind tunnel. Then  $C_D$  is calculated using Eq. (11.5) written as follows:

$$C_D = \frac{F_D}{A_p \rho V_0^2 / 2} \quad (11.6)$$

Much of the data ( $C_D$  versus  $Re$ ) found in the literature is obtained in this manner.

The coefficient of drag for the flat plate normal to the free stream and for other two-dimensional bodies, for a wide range of Reynolds numbers, is given in Fig. 11.5. In general, the total drag of a blunt body is partly due to viscous resistance and partly due to pressure variation. The pressure drag is largely a function of the form or shape of the body; hence it is called form drag. The viscous drag is often called skin-friction drag.

#### example 11.1



A television-transmitting antenna is on top of a pipe 30 m high (98.4 ft) and 30 cm (11.8 in.) in diameter, which is on top of a tall building. What will be the total drag of the pipe and the bending moment at the base of the pipe in a 35-m/s (115-ft/s) wind at normal atmospheric pressure and a temperature of 20°C (68°F)?



**Solution** For the conditions given, the viscosity and density of the air are obtained from the Appendix:

$$\mu = 1.81 \times 10^{-5} \text{ N} \cdot \text{s}/\text{m}^2 \quad (3.78 \times 10^{-7} \text{ lbf} \cdot \text{s}/\text{ft}^2)$$

$$\rho = 1.20 \text{ kg}/\text{m}^3 \quad (0.00234 \text{ slugs}/\text{ft}^3)$$

Next the Reynolds number is calculated:

$$\text{Re} = \frac{V_0 d \rho}{\mu} = \frac{35 \text{ m/s} \times 0.30 \text{ m} \times 1.20 \text{ kg}/\text{m}^3}{(1.81 \times 10^{-5} \text{ N} \cdot \text{s}/\text{m}^2)} = 7.0 \times 10^5$$

$\checkmark$   
 $\approx 1.51 \times 10^{-5} \frac{\text{m}^2}{\text{s}}$

Then, from Fig. 11.5,  $C_D = 0.20$ . Now we compute the total drag:

$$F_D = \frac{C_D A_p \rho V_0^2}{2}$$

$$= \frac{(0.2)(30 \text{ m})(0.3 \text{ m})(1.20 \text{ kg}/\text{m}^3)(35^2 \text{ m}^2/\text{s}^2)}{2} = 1323 \text{ N}$$

Assuming that the resultant drag force acts midway up the pole, the moment is

$$M = F_D \left( \frac{L}{2} \right) = (1323 \text{ N}) \left( \frac{30}{2} \text{ m} \right) = 19,845 \text{ N} \cdot \text{m}$$

**Traditional units:**

$$F_D = 0.2(98.4 \text{ ft}) \left( \frac{11.8}{12} \text{ ft} \right) (0.00234 \text{ slugs}/\text{ft}^3) \left( \frac{115^2 \text{ ft}^2/\text{s}^2}{2} \right) = 299 \text{ lbf}$$

$$M = (299 \text{ lbf}) \left( \frac{98.4}{2} \text{ ft} \right) = 14,700 \text{ ft} \cdot \text{lbf}$$

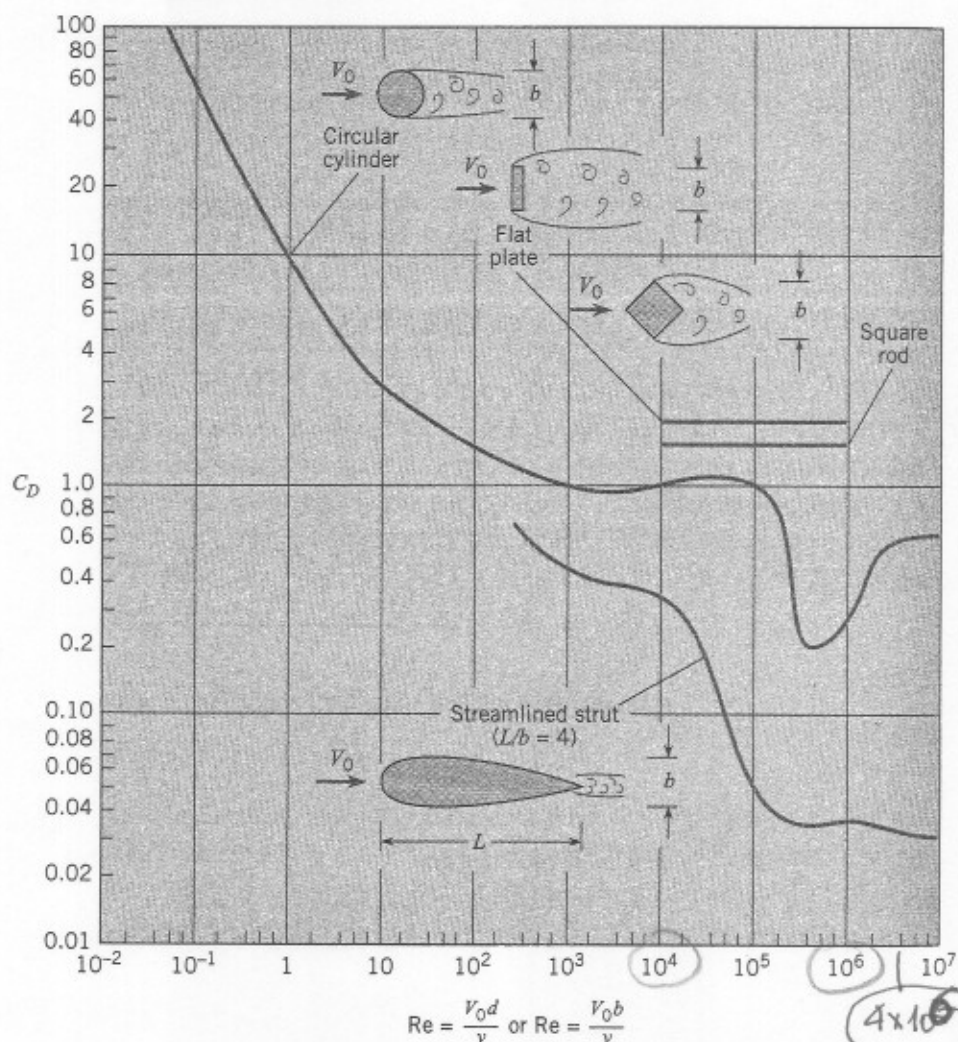
## Discussion of $C_D$ for Two-Dimensional Bodies

At low Reynolds numbers,  $C_D$  changes with the Reynolds number. The change is due to the relative change in viscous resistance, which has already been mentioned in Chapter 8. Above  $\text{Re} = 10^4$ , the flow pattern remains virtually unchanged, thereby producing constant values of  $C_p$  over the body. Constancy of  $C_p$  at high Reynolds numbers is reflected in the constancy of  $C_D$ . This characteristic, the constancy of  $C_D$  at high values of  $\text{Re}$ , is representative of most bodies that have angular form. However, certain bodies with rounded form, such as circular cylinders, show a remarkable decrease in  $C_D$  with an increase in  $\text{Re}$  from about  $10^5$  to  $5 \times 10^5$ .

This reduction in  $C_D$  at a Reynolds number of approximately  $10^5$  is due to a change in the flow pattern triggered by a change in the character of the boundary layer. For Reynolds numbers less than  $10^5$ , the boundary layer is laminar, and separation occurs about midway between the upstream side and downstream

FIGURE 11.5

Coefficient of drag versus Reynolds number for two-dimensional bodies. [Data sources: Bullivant (5), Defoe (9), Goett and Bullivant (12), Jacobs (15), Jones (17), and Lindsey (21)]



side of the cylinder (Fig. 11.6). Hence the entire downstream half of the cylinder is exposed to a relatively low pressure, which in turn produces a relatively high value for  $C_D$ . When the Reynolds number is increased to about  $10^5$ , the boundary layer on the surface of the cylinder becomes turbulent, which causes higher-velocity fluid to be mixed into the region close to the wall of the cylinder. As a consequence of the presence of this high-velocity, high-momentum fluid in the boundary layer, the flow proceeds farther downstream along the surface of the cylinder against the adverse pressure before separation occurs (Fig. 11.7).

FIGURE 11.6

Flow pattern around a cylinder for  $10^3 < Re < 10^5$ .

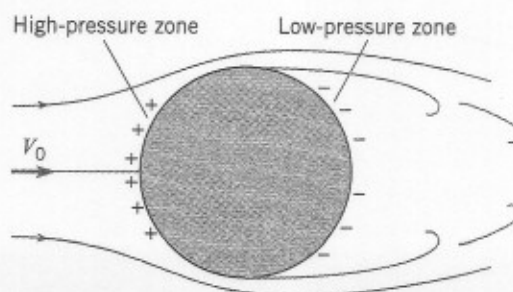
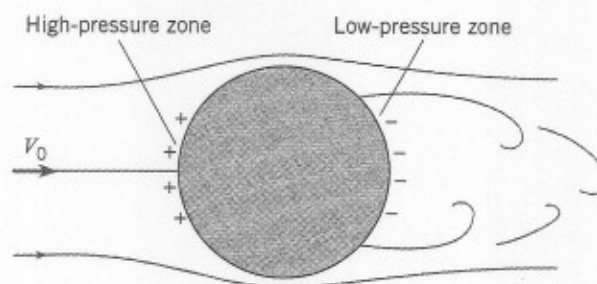


FIGURE 11.7

Flow pattern around a  
cylinder for  
 $Re > 5 \times 10^5$ .



Hence the flow pattern causes  $C_D$  to be reduced for the following reason: with the turbulent boundary layer, the streamlines downstream of the cylinder midsection diverge somewhat before separation, and hence a decrease in velocity occurs before separation. According to the Bernoulli equation, the decrease in velocity produces a pressure at the point of separation that is greater than the pressure at the midsection. Thus the pressure at the point of separation, and also in the zone of separation, is significantly greater under these conditions than when separation occurs farther upstream. Therefore, the pressure difference between the upstream and downstream surfaces of the cylinder is less at high values of  $Re$ , yielding a lower drag and a lower  $C_D$ .

Because the boundary layer is so thin, it is also very sensitive to other conditions. For example, if the surface of the cylinder is slightly roughened upstream of the midsection, the boundary layer will be forced to become turbulent at lower Reynolds numbers than those for a smooth cylinder surface. The same trend can also be produced by creating abnormal turbulence in the approach flow. The effects of roughness are shown in Fig. 11.8 for cylinders that were roughened with sand grains of size  $k$ . A small to medium size of roughness ( $10^{-3} < k/d < 10^{-2}$ ) on a cylinder triggers an early onset of reduction of  $C_D$ . However, when the relative roughness is quite large ( $10^{-2} < k/d$ ), the characteristic dip in  $C_D$  is absent.

## 11.3

## Vortex Shedding from Cylindrical Bodies

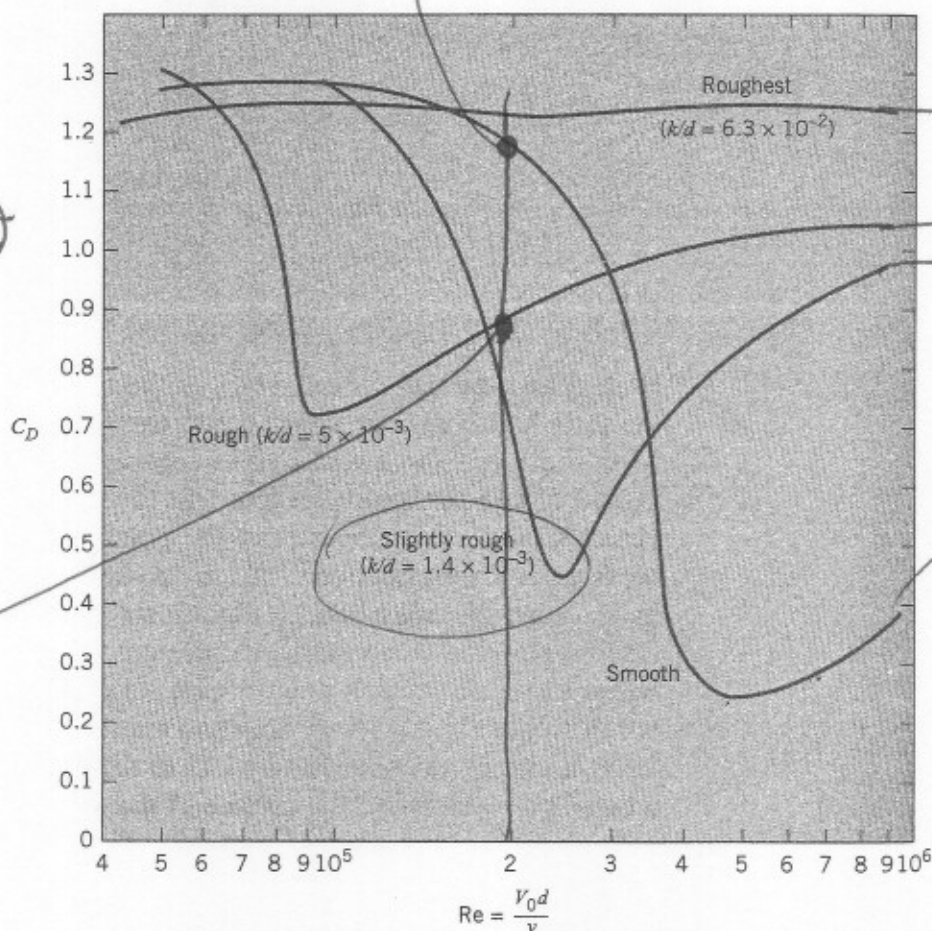
Figures 11.6 and 11.7 show the average (temporal mean) flow pattern around a cylinder. The phenomenon becomes more complex, however, when we observe the detailed flow pattern as time passes. Observations show that above  $Re \approx 50$ , vortices are formed and shed periodically downstream of the cylinder. Hence, at a given time, the detailed flow pattern might appear as in Fig. 11.9. In this figure a vortex is in the process of formation near the top of the cylinder. Below and to the right of the first vortex is another vortex, which was formed and shed a short time before. Thus the flow process in the wake of a cylinder involves the formation and shedding of vortices alternately from one side and then the other. This phenomenon is of major importance in engineering design, because the alternate formation and shedding of vortices also creates a regular change in pressure with consequent periodicity in side thrust on the cylinder. Vortex shedding was



Total drag = frictional + form drag

FIGURE 11.8

Effects of roughness on  $C_D$  for a cylinder. [After Miller et al. (22)]



the primary cause of failure of the Tacoma Narrows suspension bridge in the state of Washington in 1940. Another, more commonplace effect of vortex shedding is the "singing" of wires in the wind.

If the frequency of the vortex shedding is in resonance with the natural frequency of the member that produces it, large amplitudes of vibration with resulting large stresses can develop. Experiments show that the frequency of shedding is given in terms of the Strouhal number  $St$ , and this in turn is a function of the Reynolds number. Here the Strouhal number is defined as

$$St = \frac{nd}{V_0} \quad (11.7)$$

where  $n$  is the frequency of shedding of vortices from one side of the cylinder, in Hz,  $d$  is the diameter of the cylinder, and  $V_0$  is the free-stream velocity.

FIGURE 11.9

Formation of a vortex behind a cylinder.



The relationship between the Strouhal number and the Reynolds number for vortex shedding from a circular cylinder is given in Fig. 11.10.

Other cylindrical and two-dimensional bodies also shed vortices. Consequently, the engineer should always be alert to vibration problems when designing structures that are exposed to wind or water flow.

### example 11.2

For the cylinder and conditions of Example 11.1, at what frequency will the vortices be shed?

**Solution** We compute the frequency  $n$  from the Strouhal number, which is given in Fig. 11.10 as a function of the Reynolds number. Thus with a Reynolds number of  $7.0 \times 10^5$  from Example 11.1, we read a Strouhal number of 0.23. But

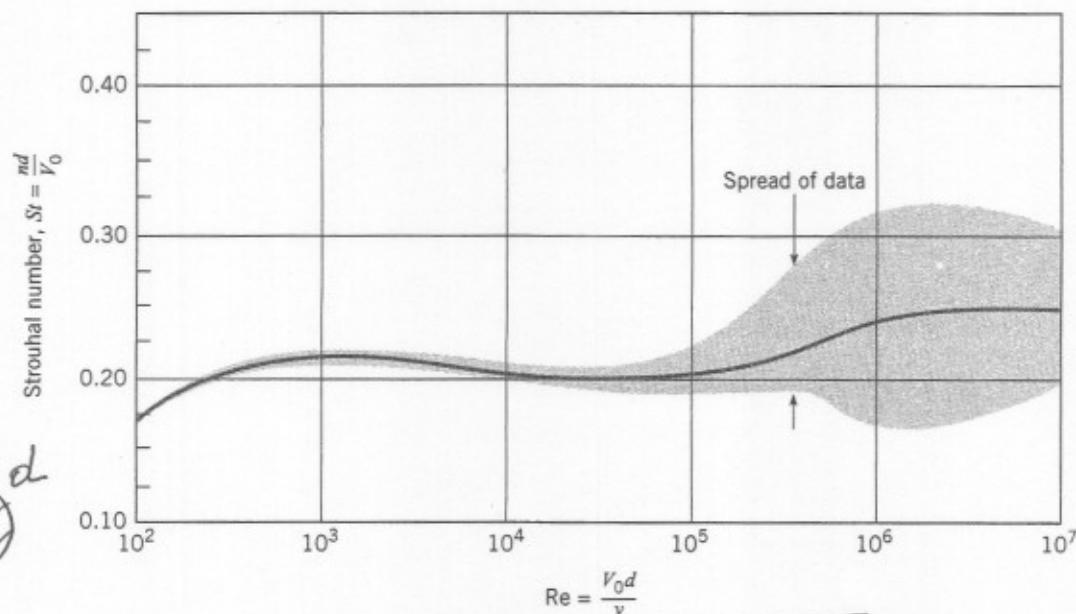
$$St = \frac{nd}{V_0}$$

so

$$n = \frac{SV_0}{d} = \frac{0.23 \times 35 \text{ m/s}}{0.30 \text{ m}} = 27 \text{ Hz}$$

FIG. 11.10

Strouhal number versus Reynolds number for flow past a circular cylinder. [After Jones (17) and Roshko (27)]



### 11.4

## Effect of Streamlining

$$\text{Strouhal } No = \frac{n \cdot d}{V_0} \quad (St)$$

For Reynolds numbers greater than  $10^3$ , the drag of a cylinder is predominantly due to the pressure variation around the cylinder. The pressure difference between



the upstream and downstream sides of the cylinder is the primary cause of drag, and this pressure difference is due largely to separation. Hence, if the separation can be eliminated, the drag will be reduced. That is exactly what streamlining does. Streamlining reduces the extreme curvature on the downstream side of the body, and this process reduces or eliminates separation. Therefore, the coefficient of drag is greatly reduced, as seen in Fig. 11.5 ( $C_D$  for the streamlined shape is only about 10% of  $C_D$  for the circular cylinder when  $Re \approx 5 \times 10^5$ ).

When a body is streamlined by elongating it and reducing its curvature, the pressure drag is reduced. However, the viscous drag is increased because there is a greater amount of surface on the streamlined body than on the non-streamlined body. Consequently, when a body is streamlined to produce minimum drag, there is an optimum condition to be sought. The optimum condition results when the sum of surface drag and pressure drag is minimum.

In this discussion of streamlining, it is interesting to note that streamlining to produce minimum drag at high Reynolds numbers will probably not produce minimum drag at very low Reynolds numbers. For Reynolds numbers less than unity, the majority of the drag of a cylinder is due to the viscous shear stress on the wall of the cylinder. Hence, if the cylinder is streamlined, the viscous shear stress is simply magnified and  $C_D$  may actually increase for this range of  $Re$  where the viscous resistance is predominant.

At high values of the Reynolds number, another advantage of streamlining is that the periodic formation of vortices is eliminated.

### example 11.3

Compare the drag of the cylinder of Example 11.1. with the drag of the streamlined shape shown in Fig. 11.5. Assume that they both have the same projected area and that the streamlined shape is oriented for minimum drag.

**Solution** Because  $F_D = C_D A_p \rho V_0^2 / 2$ , the drag of the streamlined shape will be

$$F_{DS} = F_{DC} \left( \frac{C_{DS}}{C_{DC}} \right)$$

where  $F_{DS}$  is the drag of the streamlined shape,  $F_{DC}$  is the drag of the cylinder,  $C_{DS}$  is the coefficient of drag of the streamlined shape, and  $C_{DC}$  is the coefficient of drag of the cylinder. But  $C_{DS} = 0.034$ , from Fig. 11.5 with  $Re = 7.0 \times 10^5$ . Then

$$F_{DS} = F_{DC} \left( \frac{0.034}{0.20} \right) = (1323 \text{ N}) \left( \frac{0.034}{0.20} \right)$$

$$F_{DS} = 225 \text{ N}$$

$$\frac{F_{DS}}{F_{DC}} = 0.17$$

## 11.5

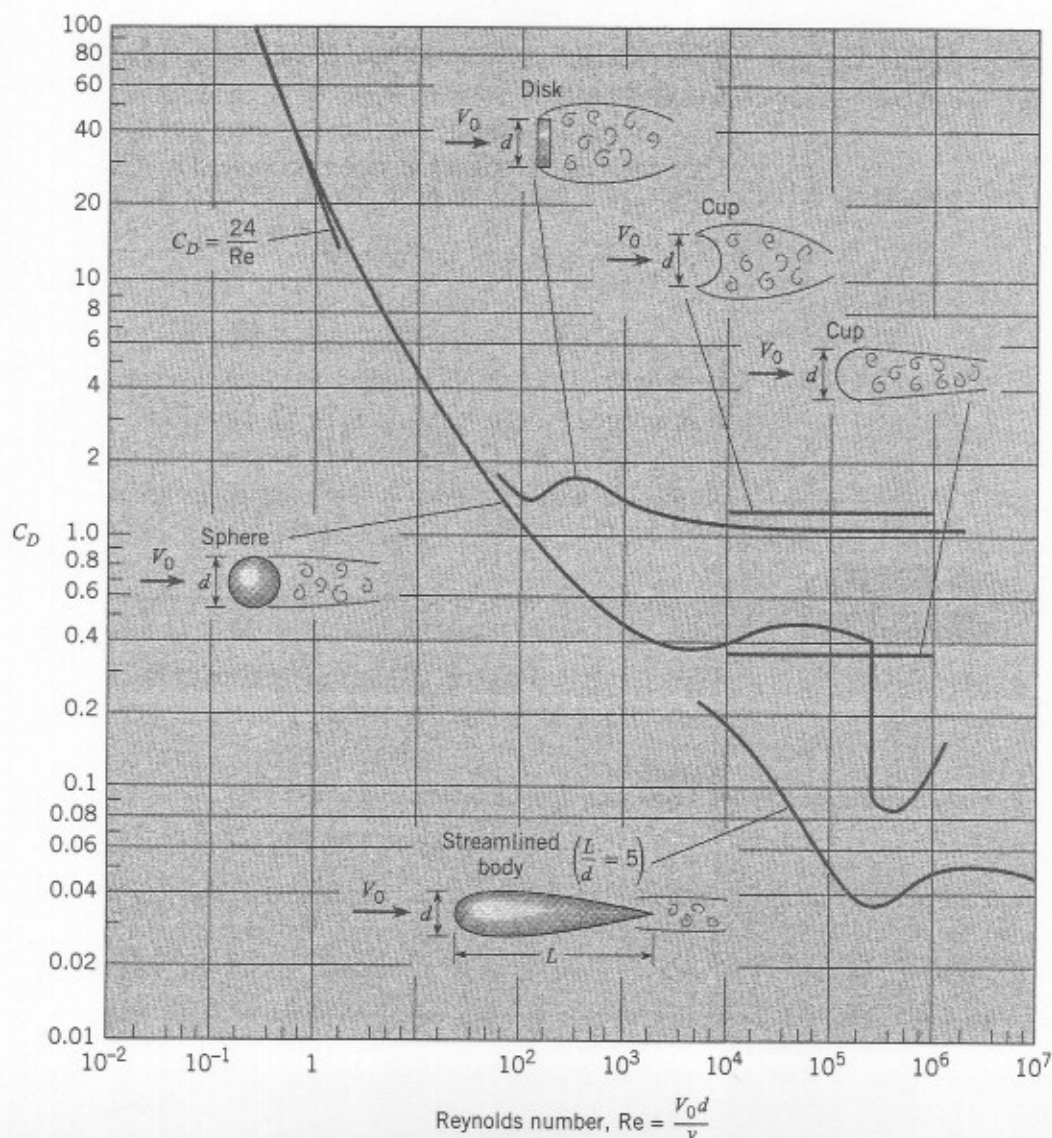
## Drag of Axisymmetric and Three-Dimensional Bodies

The same principles that apply to the drag of two-dimensional bodies also apply to that of axisymmetric and three-dimensional bodies. That is, at very low values of the Reynolds number, the coefficient of drag is given by exact equations relating  $C_D$  and  $Re$ . At high values of  $Re$ , the coefficient of drag becomes constant for angular bodies, whereas rather abrupt changes in  $C_D$  occur for rounded bodies. All of these characteristics can be seen in Fig. 11.11, where  $C_D$  is plotted against  $Re$  for several axisymmetric bodies.

The drag coefficient of a sphere is of special interest because many applications involve the drag of spherical or near-spherical objects such as particles

FIGURE 11.11

Coefficient of drag  
versus Reynolds number  
for axisymmetric bodies.  
[Data sources: Abbott  
(1), Voort and Joyner  
(4), Freeman (11), and  
Rouse (28)]



and droplets. Also, the drag of a sphere is often used as a standard of comparison for other shapes. For Reynolds numbers less than 0.5, the flow around the sphere is laminar and amenable to analytical solutions. An exact solution by Stokes yielded the following equation, which is called *Stokes' law*, for the drag of a sphere:

$$F_D = 3\pi\mu V_0 d \quad (11.8)$$

Note that the drag for this laminar-flow condition varies directly with the first power of  $V_0$ . This is characteristic of all laminar-flow processes. For completely turbulent flow, the drag is a function of the velocity to the second power. When Eqs. (11.8) and (11.6) are solved simultaneously, we get the coefficient of drag corresponding to Stokes' law:

$$C_D = \frac{24}{\text{Re}} \quad (11.9)$$

Thus for flow past a sphere, when  $\text{Re} \leq 0.5$ , one may use the direct relation for  $C_D$  given above.

Several correlations for the drag coefficient of a sphere are available (7). One such correlation has been proposed by Cliff and Gauvin (6):

$$C_D = \frac{24}{\text{Re}}(1 + 0.15\text{Re}^{0.687}) + \frac{0.42}{1 + 4.25 \times 10^4 \text{Re}^{-1.16}} \quad (11.10)$$

which deviates from the *standard drag curve*\* by  $-4\%$  to  $6\%$  for Reynolds numbers up to  $3 \times 10^5$ . Note that as Reynolds number approaches zero, this correlation reduces to the equation for Stokes flow.

Values for  $C_D$  for other axisymmetric and three-dimensional bodies at high Reynolds numbers ( $\text{Re} > 10^4$ ) are given in Table 11.1.

#### example 11.4

What is the drag of a 12-mm sphere that drops at a rate of 8 cm/s in oil ( $\mu = 10^{-1} \text{ N} \cdot \text{s}/\text{m}^2$ ,  $S = 0.85$ )?

**Solution**

$$\rho = 0.85 \times 1000 \text{ kg}/\text{m}^3$$

$$\text{Then } \text{Re} = \frac{Vd\rho}{\mu} = \frac{(0.08 \text{ m/s})(0.012 \text{ m})(850 \text{ kg}/\text{m}^3)}{10^{-1} \text{ N} \cdot \text{s}/\text{m}^2} = 8.16$$

\* The *standard drag curve* represents the best fit of the cumulative data that have been obtained for drag coefficient of a sphere.



Next, from Fig. 11.11,

$$C_D = 5.3$$

$$F_D = \frac{C_D A_p \rho V_0^2}{2}$$

$$\begin{aligned} \text{Hence } F_D &= \frac{(5.3)(\pi/4)(0.012^2 \text{ m}^2)(850 \text{ kg/m}^3)(0.08^2 \text{ m}^2/\text{s}^2)}{2} \\ &= 1.63 \times 10^{-3} \text{ N} \end{aligned}$$

◁

### example 11.5

A bicyclist travels on a level path. The frontal area of the cyclist and bicycle is  $2 \text{ ft}^2$  and the drag coefficient is 0.8. The density of the air is  $0.075 \text{ lbm/ft}^3$ . The physiological limit of power for this well-trained cyclist is 0.5 hp. Neglecting rolling friction, find the maximum speed of the cyclist.

**Solution** The power is the product of the drag force and the velocity.

$$P = F_D V = (1/2) C_D A_p \rho V^3$$

Solving for the velocity, we get

$$\begin{aligned} V &= (2P/\rho C_D A_p)^{1/3} \\ &= \left[ \frac{2 \times 0.5 \text{ hp} \times 550 \text{ ft-lbf/s hp}}{0.075 \text{ lbm/ft}^3 \times (1/32.2) \text{ slugs/lbm} \times 0.8 \times 2 \text{ ft}^2} \right]^{1/3} \\ &= 52.8 \text{ ft/s} = 36.0 \text{ mph} \end{aligned}$$

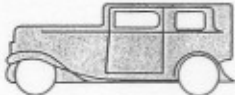

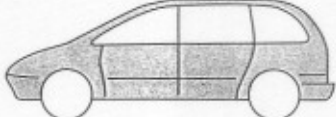
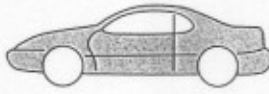



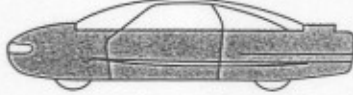

◁

## 11.6

### Terminal Velocity

The engineer is often required to use drag data in the computation of the *terminal velocity* of a body. When a body is first dropped in the atmosphere or in water, it accelerates under the action of its weight. Then, as the speed of the body increases, the drag increases. Finally, the drag reaches a magnitude such that the sum of all external forces on the body is zero. Hence acceleration ceases, and the body has attained its terminal velocity. Thus the terminal velocity is the maximum velocity attained by a falling body. This assumes that the fluid

TABLE II.2 COEFFICIENTS OF DRAG FOR CARS

Make and Model	Profile	$C_D$
1932 Fiat Balillo		0.60
Volkswagen "Bug"		0.46
Plymouth Voyager		0.36
Toyota Paseo		0.31
Dodge Intrepid		0.31
Ford Taurus		0.30
Mercedes-Benz E320		0.29
Ford Probe V (concept car)		0.14
GM Sunraycer (experimental solar vehicle)		0.12

$A_p$  = projected area



Drag force =

$$= \frac{1}{2} \rho v^2 A_p C_D$$

$C_D$  = drag coefficient

most streamlined cars was the "Bluebird," which set a world land-speed record in 1938. Its  $C_D$  was 0.16. The minimum  $C_D$  of well-streamlined racing cars is about 0.20. Thus, lowering the  $C_D$  for passenger cars below 0.30 will require exceptional design and workmanship. For example, the underside of most cars is aerodynamically very rough (axles, wheels, muffler, fuel tank, shock absorbers, and so on). One way to smooth the underside is to add a panel to the bottom of the car. But then clearance may become a problem, and adequate dissipation of heat from the muffler may be hard to achieve. Other basic features of the automobile that contribute to drag but are not very amenable to drag-reduction modifications are

H<sub>2</sub>O

TABLE A.5 APPROXIMATE PHYSICAL PROPERTIES OF WATER\* AT ATMOSPHERIC PRESSURE

Temperature	Density	Specific weight	Dynamic viscosity	Kinematic viscosity	Vapor pressure
	kg/m <sup>3</sup>	N/m <sup>3</sup>	N·s/m <sup>2</sup>	m <sup>2</sup> /s	N/m <sup>2</sup> abs.
0°C	1000	9810	$1.79 \times 10^{-3}$	$1.79 \times 10^{-6}$	611
5°C	1000	9810	$1.51 \times 10^{-3}$	$1.51 \times 10^{-6}$	872
10°C	1000	9810	$1.31 \times 10^{-3}$	$1.31 \times 10^{-6}$	1230
15°C	999	9800	$1.14 \times 10^{-3}$	$1.14 \times 10^{-6}$	1700
20°C	998	9790	$1.00 \times 10^{-3}$	$1.00 \times 10^{-6}$	2340
25°C	997	9781	$8.91 \times 10^{-4}$	$8.94 \times 10^{-7}$	3170
30°C	996	9771	$7.97 \times 10^{-4}$	$8.00 \times 10^{-7}$	4250
35°C	994	9751	$7.20 \times 10^{-4}$	$7.24 \times 10^{-7}$	5630
40°C	992	9732	$6.53 \times 10^{-4}$	$6.58 \times 10^{-7}$	7380
50°C	988	9693	$5.47 \times 10^{-4}$	$5.53 \times 10^{-7}$	12,300
60°C	983	9643	$4.66 \times 10^{-4}$	$4.74 \times 10^{-7}$	20,000
70°C	978	9594	$4.04 \times 10^{-4}$	$4.13 \times 10^{-7}$	31,200
80°C	972	9535	$3.54 \times 10^{-4}$	$3.64 \times 10^{-7}$	47,400
90°C	965	9467	$3.15 \times 10^{-4}$	$3.26 \times 10^{-7}$	70,100
100°C	958	9398	$2.82 \times 10^{-4}$	$2.94 \times 10^{-7}$	101,300

	slugs/ft <sup>3</sup>	lbf/ft <sup>3</sup>	lbf·s/ft <sup>2</sup>	ft <sup>2</sup> /s	psia
40°F	1.94	62.43	$3.23 \times 10^{-5}$	$1.66 \times 10^{-5}$	0.122
50°F	1.94	62.40	$2.73 \times 10^{-5}$	$1.41 \times 10^{-5}$	0.178
60°F	1.94	62.37	$2.36 \times 10^{-5}$	$1.22 \times 10^{-5}$	0.256
70°F	1.94	62.30	$2.05 \times 10^{-5}$	$1.06 \times 10^{-5}$	0.363
80°F	1.93	62.22	$1.80 \times 10^{-5}$	$0.930 \times 10^{-5}$	0.506
100°F	1.93	62.00	$1.42 \times 10^{-5}$	$0.739 \times 10^{-5}$	0.949
120°F	1.92	61.72	$1.17 \times 10^{-5}$	$0.609 \times 10^{-5}$	1.69
140°F	1.91	61.38	$0.981 \times 10^{-5}$	$0.514 \times 10^{-5}$	2.89
160°F	1.90	61.00	$0.838 \times 10^{-5}$	$0.442 \times 10^{-5}$	4.74
180°F	1.88	60.58	$0.726 \times 10^{-5}$	$0.385 \times 10^{-5}$	7.51
200°F	1.87	60.12	$0.637 \times 10^{-5}$	$0.341 \times 10^{-5}$	11.53
212°F	1.86	59.83	$0.593 \times 10^{-5}$	$0.319 \times 10^{-5}$	14.70

\*Notes: (1) Bulk modulus  $E_v$  of water is approximately  $2.2 \text{ GPa}$  ( $3.2 \times 10^5 \text{ psi}$ ); (2) water-air surface tension is approximately  $7.3 \times 10^{-2} \text{ N/m}$  ( $5 \times 10^{-3} \text{ lbf/ft}$ ) from 10°C to 50°C.

SOURCE: Reprinted with permission from R. E. Bolz and G. L. Tuve, *Handbook of Tables for Applied Engineering Science*, CRC Press, Inc., Cleveland, 1973. Copyright © 1973 by The Chemical Rubber Co., CRC Press, Inc.



Air

TABLE A.3 MECHANICAL PROPERTIES OF AIR AT STANDARD ATMOSPHERIC PRESSURE

Temperature	Density	Specific weight	Dynamic viscosity	Kinematic viscosity
	kg/m <sup>3</sup>	N/m <sup>3</sup>	N · s/m <sup>2</sup>	m <sup>2</sup> /s
-20°C	1.40	13.7	$1.61 \times 10^{-5}$	$1.16 \times 10^{-5}$
-10°C	1.34	13.2	$1.67 \times 10^{-5}$	$1.24 \times 10^{-5}$
0°C	1.29	12.7	$1.72 \times 10^{-5}$	$1.33 \times 10^{-5}$
10°C	1.25	12.2	$1.76 \times 10^{-5}$	$1.41 \times 10^{-5}$
20°C	1.20	11.8	$1.81 \times 10^{-5}$	$1.51 \times 10^{-5}$
30°C	1.17	11.4	$1.86 \times 10^{-5}$	$1.60 \times 10^{-5}$
40°C	1.13	11.1	$1.91 \times 10^{-5}$	$1.69 \times 10^{-5}$
50°C	1.09	10.7	$1.95 \times 10^{-5}$	$1.79 \times 10^{-5}$
60°C	1.06	10.4	$2.00 \times 10^{-5}$	$1.89 \times 10^{-5}$
70°C	1.03	10.1	$2.04 \times 10^{-5}$	$1.99 \times 10^{-5}$
80°C	1.00	9.81	$2.09 \times 10^{-5}$	$2.09 \times 10^{-5}$
90°C	0.97	9.54	$2.13 \times 10^{-5}$	$2.19 \times 10^{-5}$
100°C	0.95	9.28	$2.17 \times 10^{-5}$	$2.29 \times 10^{-5}$
120°C	0.90	8.82	$2.26 \times 10^{-5}$	$2.51 \times 10^{-5}$
140°C	0.85	8.38	$2.34 \times 10^{-5}$	$2.74 \times 10^{-5}$
160°C	0.81	7.99	$2.42 \times 10^{-5}$	$2.97 \times 10^{-5}$
180°C	0.78	7.65	$2.50 \times 10^{-5}$	$3.20 \times 10^{-5}$
200°C	0.75	7.32	$2.57 \times 10^{-5}$	$3.44 \times 10^{-5}$

	slugs/ft <sup>3</sup>	lbf/ft <sup>3</sup>	lbf · s/ft <sup>2</sup>	ft <sup>2</sup> /s
0°F	0.00269	0.0866	$3.39 \times 10^{-7}$	$1.26 \times 10^{-4}$
20°F	0.00257	0.0828	$3.51 \times 10^{-7}$	$1.37 \times 10^{-4}$
40°F	0.00247	0.0794	$3.63 \times 10^{-7}$	$1.47 \times 10^{-4}$
60°F	0.00237	0.0764	$3.74 \times 10^{-7}$	$1.58 \times 10^{-4}$
80°F	0.00228	0.0735	$3.85 \times 10^{-7}$	$1.69 \times 10^{-4}$
100°F	0.00220	0.0709	$3.96 \times 10^{-7}$	$1.80 \times 10^{-4}$
120°F	0.00213	0.0685	$4.07 \times 10^{-7}$	$1.91 \times 10^{-4}$
150°F	0.00202	0.0651	$4.23 \times 10^{-7}$	$2.09 \times 10^{-4}$
200°F	0.00187	0.0601	$4.48 \times 10^{-7}$	$2.40 \times 10^{-4}$
300°F	0.00162	0.0522	$4.96 \times 10^{-7}$	$3.05 \times 10^{-4}$
400°F	0.00143	0.0462	$5.40 \times 10^{-7}$	$3.77 \times 10^{-4}$

SOURCE: Reprinted with permission from R. E. Bolz and G. L. Tuve, *Handbook of Tables for Applied Engineering Science*, CRC Press, Inc., Cleveland, 1973. Copyright © 1973 by The Chemical Rubber Co., CRC Press, Inc.